

1230

# Auger Electron Spectroscopy, Secondary Ion Mass Spectrometry and Optical Characterization of a-C:H and BN Films

(NASA-TM-87258) AUGER ELECTRON  
SPECTROSCOPY, SECONDARY ION MASS  
SPECTROSCOPY AND OPTICAL CHARACTERIZATION OF  
a-C-H AND BN FILMS (NASA) 13 p  
HC A02/MF A01

N86-25268

Unclass  
43045

CSCI 20L G3/76

John J. Pouch, Samuel A. Alterovitz,  
and Joseph D. Warner  
*Lewis Research Center*  
*Cleveland, Ohio*

Prepared for the  
Symposium on Plasma Processing at the  
Spring Meeting of the Materials Research Society  
Palo Alto, California, April 15-18, 1986

**NASA**



AUGER ELECTRON SPECTROSCOPY, SECONDARY ION MASS SPECTROSCOPY AND OPTICAL  
CHARACTERIZATION OF a-C:H AND BN FILMS

John J. Pouch, Samuel A. Alterovitz, and Joseph D. Warner  
National Aeronautics and Space Administration  
Lewis Research Center  
Cleveland, Ohio 44135

SUMMARY

The amorphous dielectrics a-C:H and BN were deposited on III-V semiconductors. Optical band gaps as high as 3 eV were measured for a-C:H generated by C<sub>4</sub>H<sub>10</sub> plasmas; a comparison was made with band gaps obtained from films prepared by CH<sub>4</sub> glow discharges. The ion beam deposited BN films exhibited amorphous behavior with band gaps on the order of 5 eV.

Film compositions were studied by Auger electron spectroscopy (AES), x-ray photoelectron spectroscopy (XPS) and secondary ion mass spectrometry (SIMS). The optical properties were characterized by ellipsometry, UV/VIS absorption, and IR reflection and transmission. Etching rates of a-C:H subjected to O<sub>2</sub> discharges were determined.

INTRODUCTION

Thin dielectric films can be useful for semiconductor passivation, insulation, and encapsulation. In view of the rapid advances that have been made in very high speed digital and microwave integrated circuits development, there is a continuing need to deposit and characterize a variety of films in order to meet the stringent requirements of the technology.

Amorphous hydrogenated carbon (a-C:H) (refs. 1 to 13) and boron nitride (BN) (refs. 14 to 20) films exhibit properties which may be suitable for semiconductor applications. In the case of a-C:H, hard, transparent, homogeneous films can be prepared on different substrates. Electrical resistivities as high as 10<sup>15</sup> Ω-cm and breakdown fields as high as 10<sup>7</sup> V/cm are achievable (ref. 10). The deposits can withstand aggressive chemical environments (ref. 11). The optical energy gap is sensitive to the deposition parameters. Hard, transparent BN films can be formed on various materials. BN, a high temperature dielectric, is a promising candidate for insulation, masking, and passivation.

In the present study, we report on the film compositions of a-C:H and BN using Auger electron spectroscopy (AES), x-ray photoelectron spectroscopy (XPS) and secondary ion mass spectrometry (SIMS). Optical properties are obtained by ellipsometry, UV/VIS spectrophotometry, and IR reflection and transmission.

EXPERIMENTAL

a-C:H films were deposited on Si, quartz, GaAs, and InP. The substrates were placed on the grounded anode of the parallel plate reactor; the upper

electrode was capacitively coupled to the 30 kHz power source. Methane or butane glow discharges were generated for the experiments.

Low energy (150 eV) ion beam deposition utilizing borazine produced thin BN films on Si and quartz for two temperatures: 200 and 350 °C. Attempts to deposit BN on GaAs, InP and Ge were unsuccessful due to adhesion problems.

Compositional depth profiles of the a-C:H and BN samples were obtained by AES and SIMS. Both methods utilized 3 keV Ar ions for sputtering.

An Al anode, subjected to 10 keV electron bombardment, provided the  $K_{\alpha}$  radiation for XPS measurements. The Au 4f<sub>7/2</sub> line at 83.8 eV on the binding energy scale was used for referencing.

Ellipsometric studies were performed using a rotating analyzer ellipsometer. A He-Ne laser and a Hg arc lamp produced the incident light. The multiple angles and wavelengths method was applied to the experimental data (refs. 21 and 22). At least five angles of incidence were used at each wavelength. Refractive indices and extinction coefficients for Si were taken from the work of Aspnes and Studna (ref. 23).

The reflection and transmission characteristics at normal incidence were determined in the IR (2.5 to 50  $\mu\text{m}$  range) with the use of a computer controlled spectrophotometer. The sample compartment was continuously purged with dry  $\text{N}_2$ . Absorption studies in the 0.19 to 3.2  $\mu\text{m}$  range were also made by spectrophotometry. The slit width was 2 nm, and up to 200 data points were accumulated from each sample. A blank plate was positioned in the reference path for background suppression. The difference between the film and quartz plate reflectivities was not taken into account.

## RESULTS AND DISCUSSIONS

### a-C:H Films

A surface profiler was used to determine film thicknesses. The deposition rate, G, as a function of plasma power, P, for a-C:H deposited on Si is shown in figure 1. The hydrocarbon source is  $\text{C}_4\text{H}_{10}$ , and the chamber pressure is ~170 mtorr. At 150 W, a rate ~185 Å/min is attained. The results suggest that saturation occurs at the highest powers. A similar trend is observed in a-C:H deposited on InP by  $\text{CH}_4$  discharges (ref. 9); therefore, in the first approximation, deposition rates resulting from  $\text{CH}_4$  or  $\text{C}_4\text{H}_{10}$  plasmas may be described by the same chemical kinetics. However, the hydrocarbon source can have a marked effect on film properties.

Film analyses by AES and XPS show carbon to be present (ref. 8), with occasional traces of interfacial oxygen (up to 4 at %).

A SIMS depth profile of a-C:H deposited on GaAs using  $\text{C}_4\text{H}_{10}$  is presented in figure 2. The  $\text{CH}_X^+$  ( $X = 0, 1, 2, 3$ ) distributions are uniform in the film, but they drop to lower levels in the vicinity of the carbon-GaAs interface. Thus, different H-C bonds (ref. 24) are produced in the film by the plasma radicals (refs. 12 to 13). Furthermore, the oxygen level that is present in the film is not detectable by the AES technique. In addition, the  $\text{Ga}^+$  and  $\text{As}^+$

signals are higher during the first several minutes of sputtering, in contrast to the levels associated with the rest of the film. This effect can result from signal enhancement generated by adsorbed oxygen (ref. 25).

A Tauc plot, i.e.  $(AE)^{1/2}$  versus  $E$ , is shown in figure 3 for a-C:H( $C_4H_{10}$ , 150 W, 170 mtorr, 23 °C) deposited on quartz. The absorbance is  $A$ , and the photon energy is  $E$ . The band gap,  $E_0$ , is determined by fitting the absorption data (e.g. see fig. 3) to a model describing interband optical absorption in a noncrystalline solid (ref. 26). A linear relationship between  $(AE)^{1/2}$  and  $E$  is characteristic of an amorphous material.

Figure 4 summarizes the dependence of  $E_0$  on plasma power,  $P$ , for a-C:H deposited on quartz using  $CH_4$  and  $C_4H_{10}$ . In both experiments, the chamber pressure is 170 mtorr. We note that higher values of  $E_0$  (fixed  $P$ ) are achieved when depositions are made with  $C_4H_{10}$ . At 50 W, we find  $E_0 \sim 3$  eV; in contrast, the highest band gap for methane-derived films is  $\sim 1.8$  eV. Ellipsometric results on a-C:H prepared by  $C_4H_{10}$  discharges suggest that the variation in  $E_0$  versus  $P$  (see fig. 4) is related to film inhomogeneities. This concept has not been tested for a-C:H obtained from  $CH_4$  films made with a pressure of 170 mtorr.

The etch rate,  $ER$ , of a-C:H subjected to an  $O_2$  discharge (refs. 27 to 31) (etching conditions: 100 W, 170 mtorr, 23 °C, 0.5 min) was investigated. Part of each sample was protected by a Si mask. Step height measurements were made with a surface profiler. Spot check of the thickness measurement using ellipsometry was also done, confirming the surface profiling result. In figure 5,  $ER$  is plotted as a function of plasma power. The substrate is Si. (Deposition conditions:  $CH_4$ , 315 mtorr, 23 °C.) The etch rate decreases with power, indicating that the film density and/or chemical bonding is increasing. The Ar ion etching rate (3 keV) of a-C:H grown on InP (identical deposition parameters) also drops as  $P$  increases (ref. 9).

#### BN Films

An AES depth profile of ion beam deposited BN on Si is shown in figure 6 (200 °C). The film contains oxygen and carbon. The same results are obtained for the 350 °C deposition.

Analysis of the B1s lineshape by means of XPS indicates the presence of boron-nitrogen bonding. Contributions from elemental B, and  $B_2O_3$  are not detected because of the low signal-to-noise ratio.

Near surface analysis of the BN films was made by SIMS. The following ions are identified:  $B^+$ ,  $B_2^+$ ,  $C^+$ ,  $O^+$ ,  $Si^+$ ,  $Si_2^+$ , and  $SiO^+$ . The peak observed at 14 amu can result from  $N^+$ ,  $CH_2^+$  and  $Si^{2+}$ .

The reflection ( $R$  in arbitrary units) and transmission ( $T$ ) spectra for ion beam deposited BN on Si are shown in figure 7. The ion beam energy and deposition temperature are 150 eV and 200 °C, respectively. Bands at 1370 and 800  $cm^{-1}$  (associated with the B-N stretch) (ref. 17) are noted, indicating chemical BN bonds in the film. N-H and B-H bands are not

observed. The additional valleys in the transmission spectrum arise from the Si substrate (ref. 19).

A Tauc plot for an ion beam deposited BN film on quartz is indicated in figure 8 (200 °C). The absorption coefficient is  $\alpha$ . A band gap value (ref. 26) of  $(5.0 \pm 0.4)$  eV is determined. The band gap characterizing the 350 °C deposition is  $(5.1 \pm 0.4)$  eV. These results are in agreement with the values reported elsewhere (refs. 17 and 19). It is believed that  $\leq 20$  percent of the BN film exhibits the cubic structure, with the remainder being amorphous (ref. 20).

The three phase model of ellipsometry was applied to the BN optical data. The refractive index  $n$  as a function of  $\lambda$  is shown in figure 9. The extinction coefficient is either zero or vanishingly small for  $\lambda \geq 546.1$  nm, which is consistent with the absorption data (fig. 8). A decrease in  $n$  occurs as  $\lambda$  increases. In addition,  $n$  (fixed  $\lambda$ ) decreases with increasing temperature (ref. 16). The Ar ion etch rates of BN at 200 and 350 °C were calculated; the lowest etch rate is associated with the sample prepared at 200 °C, suggesting densification and/or a change in chemical bonding (relative to the 350 °C deposition).

An attempt was made to fit the ellipsometric data to a four phase model. No improvement in the fit occurs when the fourth phase is an interfacial layer. If the optical properties of the uppermost component (thickness  $\sim 100$  Å) are assumed to be different from the rest of the sample (ref. 32), the variance is decreased by a factor of 5. Numerically, the top layer has a lower refractive index. The absolute value of  $n$  (fixed  $\lambda$ ) is approximately 5 percent higher than the corresponding value (identical  $\lambda$ ) plotted in figure 9. This qualitative result is independent of the deposition temperature.

#### ACKNOWLEDGEMENTS

We thank Dr. David Liu for rewarding discussions and technical assistance, and Dr. Ward Halverson of Spire Corporation for providing the BN films.

#### REFERENCES

1. S. Aisenberg and R. Chabot, J. Appl. Phys. 42, 2953 (1971).
2. C. Weissmantel, G. Reisse, H.J. Erler, F. Henny, K. Bewilogua, U. Ebersbach, and C. Schurer, Thin Solid Films 63, 315 (1979).
3. T.J. Moravec and T.W. Orent, J. Vac. Sci. Technol. 18, 226 (1981).
4. B.A. Banks and S.K. Rutledge, J. Vac. Sci. Technol. 21, 807 (1982).
5. A.A. Khan, J.A. Woollam, Y. Chung, and B.A. Banks, IEEE Electron Dev. Lett. EDL-4, 146 (1983).
6. D. Mathine, R.O. Dillon, A.A. Khan, G. Bu-Abbud, J.A. Woollam, D.C. Liu, B.A. Banks, and S. Domitz, J. Vac. Sci. Technol. A2, 365 (1984).

7. R.O. Dillon, J.A. Woollam, and V. Katkanant, Phys. Rev. B29, 3482 (1984).
8. J. D. Warner, J.J. Pouch, S.A. Alterovitz, D.C. Liu, and W. A. Lanford, J. Vac. Sci. Technol. A3, 900 (1985).
9. J.J. Pouch, S.A. Alterovitz, J.D. Warner, D.C. Liu, and W.A. Lanford, in Thin Films: The Relationship of Structure to Properties, ed. by C.R. Aita and K.S. SreeHarsha, Mat. Res. Soc. Symp. Proc. 47, Materials Research Society, Pittsburgh, pp. 201-204 (1985).
10. J.D. Lamb and J.A. Woollam, J. Appl. Phys. 57, 5420 (1985).
11. J.A. Woollam, G.H. Bu-Abbud, J.E. Oh, P.G. Snyder, J.D. Lamb, D.C. Ingram, and A.K. Ray, Electrochem. Soc. Symp. Proc. 86-3, 289 (1986).
12. J. Wagner, Ch. Wild, F. Pohl, and P. Koidl, Appl. Phys. Lett. 48, 106 (1986).
13. K. Kobayashi, N. Mutsukura, and Y. Machi, J. Appl. Phys. 59, 910 (1986).
14. M.J. Rand and J.F. Roberts, J. Electrochem. Soc. 115, 423 (1968).
15. M. Hirayama and K. Shohno. J. Electrochem. Soc. 122, 1671 (1975).
16. S.P. Murarka, C.C. Chang, D.N.K. Wang, and T.E. Smith, J. Electrochem. Soc. 126, 1951 (1979).
17. H. Miyamoto, M. Hirose, and Y. Osaka, Jap. J. Appl. Phys. 22, L216 (1983).
18. D.C. Liu, G.J. Valco, G.G. Skebe, and V.J. Kapoor, Electrochem. Soc. Symp. Proc. 83-8, 141 (1983).
19. M.D. Wiggins, C.R. Aita, and F.S. Hickernell, J. Vac. Sci. Technol. A2, 322 (1984).
20. W. Halverson, "Protective Coatings for Optical Disks," Spire Corporation, 1984.
21. G.H. Bu-Abbud, S.A. Alterovitz, N.M. Bashara and J.A. Woollam, J. Vac. Sci. Technol. A1, 619 (1983).
22. S.A. Alterovitz, G.H. Bu-Abbud, J.A. Woollam, and D.C. Liu, J. Appl. Phys. 54, 1559 (1983).
23. D.E. Aspnes and A.A. Studna, Phys. Rev. B 27, 985 (1983).
24. A. Benninghoven, Surf. Sci. 53, 596 (1975).
25. V.P. Kolonits, M. Koltai, and D. Marton, Thin Solid Films 57, 221 (1979).

26. N.F. Mott and E.A. Davis, Electronic Processes in Noncrystalline Materials, 2nd. ed., Clarendon Press, Oxford (1979), p. 291.
27. J.F. Battey, IEEE Trans. Electron Devices ED-24, 140 (1977).
28. R.F. Reichelderfer, J.M. Welty, and J.F. Battey, J. Electrochem. Soc. 124, 1926 (1977).
29. A. Szekeres, K. Kirov, and S. Alexandrova, Phys. Stat. Solidi A 63, 371 (1981).
30. L.A. Pederson, J. Electrochem. Soc. 129, 205 (1982).
31. J. M. Cook and B. W. Benson, J. Electrochem. Soc. 130, 2459 (1983).
32. S.A. Alterovitz, G. H. Bu-Abbud, J. A. Woollam, and D. C. Liu, Phys. Stat. Sol. A 85, 69 (1984).

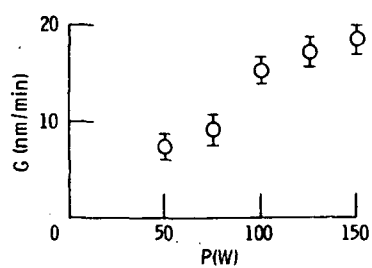


Figure 1. - Deposition rate  $G$  versus power  $P$  for  $\alpha$ -C:H film deposited on Si using  $C_4H_{10}$  discharge at 170 m Torr.

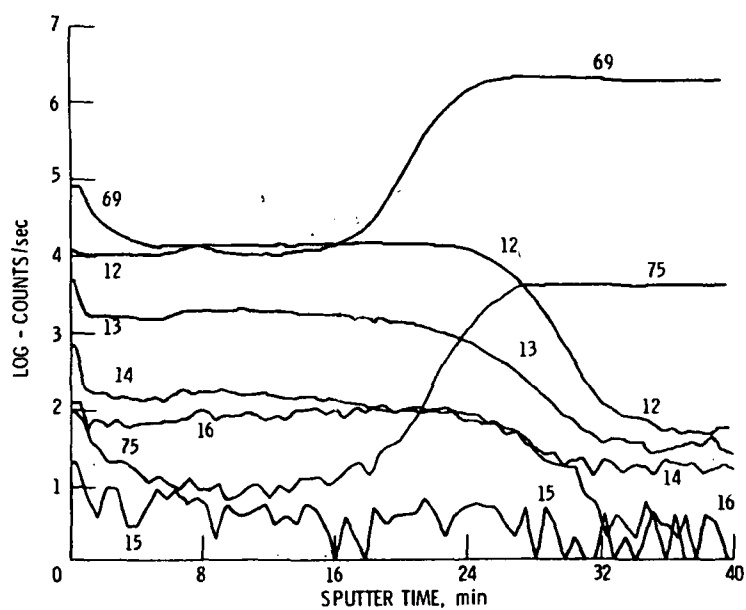


Figure 2. - SIMS depth profile of  $\alpha$ -C:H deposited on GaAs.



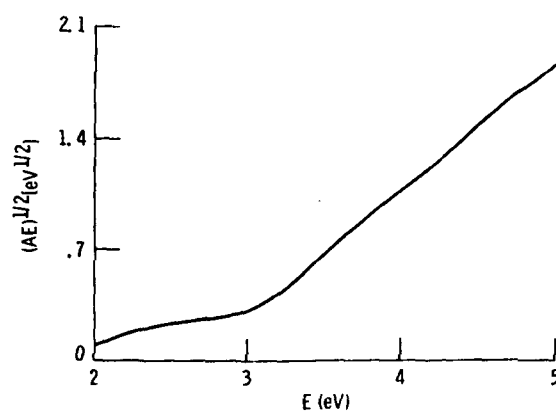


Figure 3. - Tauc plot  $(AE)^{1/2}$  versus  $E$  for  $\alpha$ -C:H deposited on quartz. Deposition parameters:  $C_4H_{10}$ , 150W, 170 m Torr.

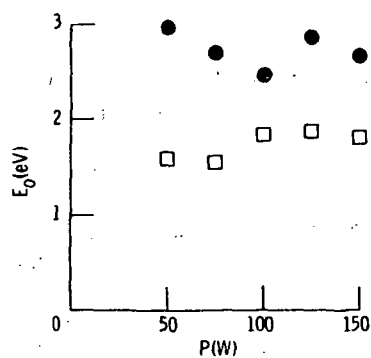


Figure 4. - Optical energy gap  $E_0$  versus deposition power  $P$  for plasma deposited  $\alpha$ -C:H on quartz using  $CH_4$  (□) and  $C_4H_{10}$  (●). The chamber pressure is 170 m Torr.

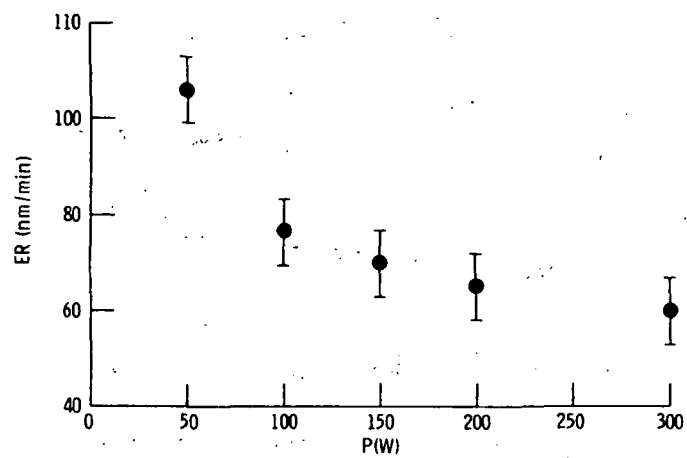


Figure 5. - Etching rate ER as a function of deposition power P for  $\alpha$ -C:H film deposited on Si. Etching parameters:  $O_2$ , 100 W, 170 m Torr, 0.5 minute.

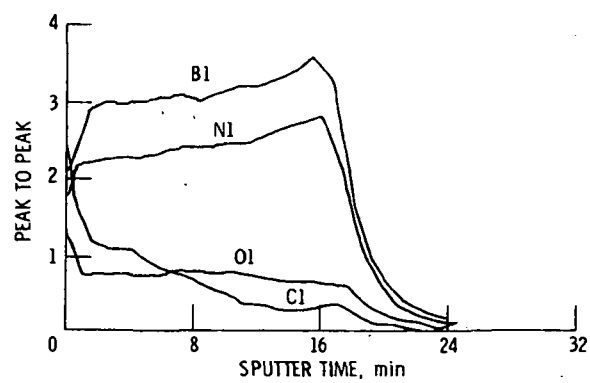


Figure 6. - AES peak to peak signal versus sputter time for ion beam deposited BN film on Si. The ion beam energy is 150 eV and the deposition temperature is 200  $^{\circ}C$ .

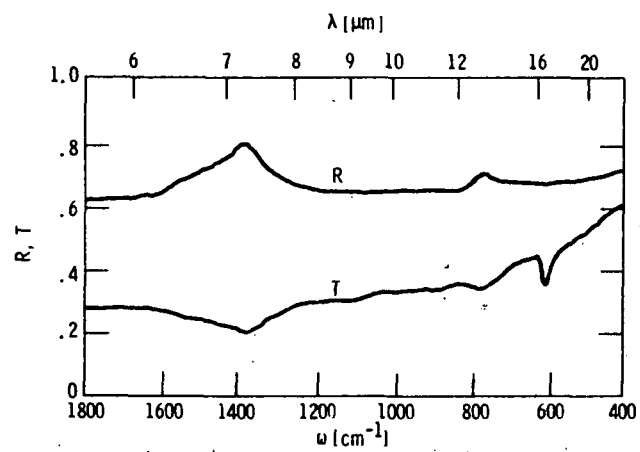


Figure 7. - Reflection  $R$  and transmission  $T$  versus wavenumber  $\omega$  for ion beam deposited BN film on Si. Deposition temperature 200  $^{\circ}\text{C}$ , ion beam energy 150 eV.

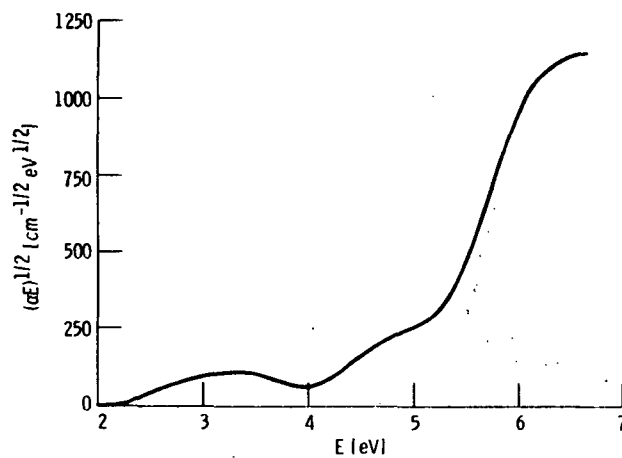


Figure 8. - Tauc plot  $(\alpha E)^{1/2}$  versus  $E$  for ion beam deposited BN film on quartz. Deposition temperature 200  $^{\circ}\text{C}$ ; ion beam energy 150 eV.

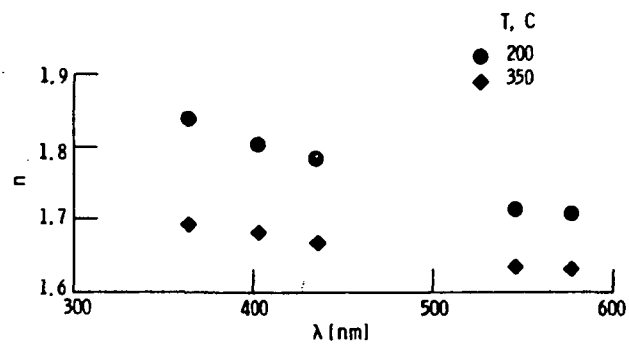


Figure 9. - Refractive index  $n$  versus wavelength  $\lambda$  for ion beam deposited BN films on Si at 2 substrate temperatures.

1. Report No. <b>NASA TM-87258</b>		2. Government Accession No.		3. Recipient's Catalog No.	
4. Title and Subtitle  <b>Auger Electron Spectroscopy, Secondary Ion Mass Spectroscopy and Optical Characterization of a-C:H and BN Films</b>				5. Report Date	
				6. Performing Organization Code <b>506-58-22</b>	
7. Author(s)  <b>John J. Pouch, Samuel A. Alterovitz, and Joseph D. Warner</b>				8. Performing Organization Report No. <b>E-2950</b>	
				10. Work Unit No.	
9. Performing Organization Name and Address  <b>National Aeronautics and Space Administration Lewis Research Center Cleveland, Ohio 44135</b>				11. Contract or Grant No.	
				13. Type of Report and Period Covered  <b>Technical Memorandum</b>	
12. Sponsoring Agency Name and Address  <b>National Aeronautics and Space Administration Washington, D.C. 20546</b>				14. Sponsoring Agency Code	
15. Supplementary Notes  <b>Prepared for the Symposium on Plasma Processing at the Spring Meeting of the Materials Research Society, Palo Alto, California, April 15-18, 1986.</b>					
16. Abstract  <b>The amorphous dielectrics a-C:H and BN were deposited on III-V semiconductors. Optical band gaps as high as 3 eV were measured for a-C:H generated by C<sub>4</sub>H<sub>10</sub> plasmas; a comparison was made with band gaps obtained from films prepared by CH<sub>4</sub> glow discharges. The ion beam deposited BN films exhibited amorphous behavior with band gaps on the order of 5 eV. Film compositions were studied by Auger electron spectroscopy (AES), x-ray photoelectron spectroscopy (XPS) and secondary ion mass spectrometry (SIMS). The optical properties were characterized by ellipsometry, UV/VIS absorption, and IR reflection and transmission. Etching rates of a-C:H subjected to O<sub>2</sub> discharges were determined.</b>					
17. Key Words (Suggested by Author(s))  <b>Carbon; Boron nitride; Plasma Semiconductors</b>			18. Distribution Statement  <b>Unclassified - unlimited STAR Category 76</b>		
19. Security Classif. (of this report) <b>Unclassified</b>		20. Security Classif. (of this page) <b>Unclassified</b>		21. No. of pages	
				22. Price*	

National Aeronautics and  
Space Administration

**Lewis Research Center**  
Cleveland, Ohio 44135

Official Business  
Penalty for Private Use \$300

SECOND CLASS MAIL

ADDRESS CORRECTION REQUESTED



Postage and Fees Paid  
National Aeronautics and  
Space Administration  
NASA-451

**NASA**

---